Materials Chemistry and Physics, 22 (1989) 281–307

TRANSITION METAL CLUSTER MATERIALS FOR MULTI-ELECTRON TRANSFER CATALYSIS

N. ALONSO-VANTE, B. SCHUBERT and H. TRIBUTSCH

Hahn-Meitner-Institut, Bereich Strahlenchemie, Glienicker Straße 100, 1000 Berlin 39 (F.R.G.)

ABSTRACT

Electrocatalytic studies on oxygen reduction and hydrogen evolution have been performed with Chevrel type cluster compounds in which both the metal within the clusters and the metal in crystal channels between clusters have systematically been changed. The main conclusion is that electronic charge carriers channelled into bimetallic interfacial clusters or cluster-metal associations provide optimal conditions for multi-electron transfer catalysis approaching the performance of platinum in acid electrolyte. The limiting factor in the case of the oxygen reduction is the interfacial instability against electrochemical desintegration of the clusters prior to reaching the thermodynamic redox potential of the reaction to be catalyzed. Molecular oxygen reduction selectivity was found with the mixed cluster in presence of methanol.

INTRODUCTION

As already outlined elsewhere [1-3] transition metal chalcogenides containing clusters of transition metals promise new oportunities in (photo)electrocatalysis of multi-electron transfer. They are expected to combine the properties of (photo)electrically conducting materials with the catalytic advantage of molecular metal-clusters which has been underlined in numerous articles and reviews [4,5]. Molecular metal clusters have, in the past, already been considered as model systems for the study of chemisorption on metal oxides and sulfides and deserve our interest already for this reason. Numerous metal cluster catalyzed reactions have already been identified. It is hoped that very special catalytic reactions may become accessible

0254-0584/89/$3.50

LeA 36388-Li.-ade

through clusters, such as unusual stereo and chemoselectivities for which the participation of more than one neighbouring metal atom is required. The possible hydration of the triple bond in CO, N_2, CN^-, RNC and RCN is also in the center of interest [6,7] since reactions of this type are successfully catalyzed on surfaces of suitable metals and metal oxides. This underlines the importance of cooperation of neighbouring metal atoms. The existance of transition metal clusters, preferentially mixed ones, within electronically conducting metal chalcogenide interfaces could combine molecular and solid state interfacial advantages which would be desirable for multi-electron transfer electrocatalysis. The little understood mechanism of oxygen reduction electrocatalysis has been the subject of initiative research in this direction [8-10].

Transition metal cluster materials for electrocatalysis

Compounds of transition metal elements of low valence states are characterized by the formation of metal-metal bonds. Organometallic molecular clusters such as, for example, $Os_3(CO)_{12}$, $Ir_4(CO)_{12}$, $Os_5(CO)_{16}$ or $Rh_6(CO)_{16}$ cannot easily be condensed to yield a conducting electrode material. However, compounds of 4d and 5d transition elements appear in the form of clusters within ionic-covalent solid state matrices [11]. Molybdenum is an example of a transition metal which forms a large variety of such cluster compounds. $Zn_2Mo_3O_8$ is one of these [12] within a series of isostructural phases of the composition $M_2Mo_3O_8$ (with M = Zn, Mn, Fe) which contains molybdenum triangles with short intracluster distances (~ 2.53 Å) as compared to metal-metal distances in Mo (2.73 Å) and has semiconducting properties. It has already been preliminarily studied in a photoelectrochemical cell [13]. Nb_3Cl_8 and $ReCl_3$ also contain these transition metal triangles. Transition metal oxides typically give rise to comparatively narrow d-energy bands due to the influence of the oxygen ligand field. Semiconducting sulfides with transition metal triangles, which would have broader d-bands, have apparently not yet been identified. Semiconducting sulfide compounds containing molybdenum tetrahedra are, for example, $FeMo_2S_4$ [14], $ZnMo_2Re_2S_8$ and $GaMo_4S_8$ [15]. In $GaMo_4S_8$ the intra-cluster distances are 2.83Å *vs* 4.06Å for the intercluster distances. The intra-cluster interaction and not the inter-cluster interaction is thus predominant for the electronic d-structure near the Fermi level. ReS_2 is a layer type semiconducting transition metal sulfide with Re_4 clusters, which has already been studied in photoelectrochemical cells [16,17].

STRUCTURE AND ELECTRONIC PROPERTIES OF CHEVREL TYPE CLUSTER MATERIALS

Cluster compounds of the Chevrel type (Mo_6X_8) contain molybdenum octahedra and form metals with the Fermi level clearly below the energy gap. For various reasons, which have been explained earlier they have been selected as model systems for (photo)electrocatalysis and need, therefore, to be explained somewhat in detail. Their crystal structure is shown in Fig. 1.

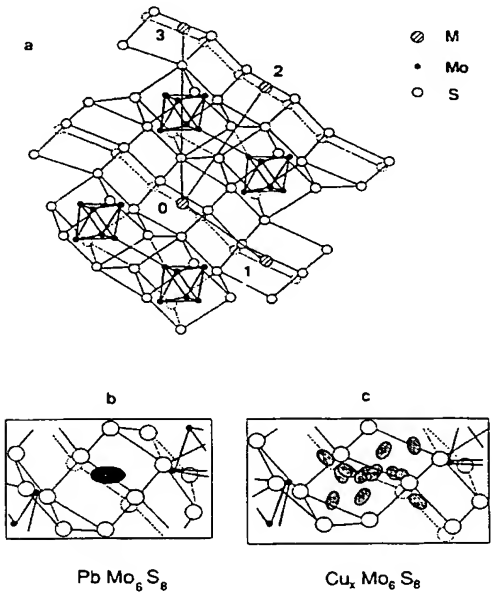

Fig. 1. (a) Crystal structure of the Mo_6X_8 units. Mo atom octahedra are shown with heavy lines and X atoms (e.g. S) by circles. $P(M)_n$, defines the position of the guest atoms, M, in the channel at the point 0. α_R is the angle $\angle 1, 0, 2$, C_H (the distance 0-3) and a_R (the distance 0-1) are also indicated. The delocalization of the metal atoms is also displayed: b) for Pb and c) Cu atoms. (adapted from ref 18a).

It clearly shows the molybdenum cluster octahedron (accomodating 20 electrons) surrounded by a cube of chalcogen atoms (e.g. sulfur) [18a]. It is also possible to distinguish the crystal channels between the clusters into which guest atoms can be inserted (at the position named $P(M)_n$ in Fig. 1). The clusters containing Chevrel phases, which include inserted guest atoms M in a composition $M_xMo_6X_8$ (X = chalcogen atom, M = metal), have been named ternary cluster materials. The compounds of formula $(MMo)_6X_8$ are named pseudo-ternary clusters, because one or more Mo atoms in the binary Mo_6X_8

are replaced by other metals (Re, Ru) as in $Mo_4Ru_2Se_8$, $Mo_2Re_4Se_8$. The channels remain unoccupied. These latter compounds and some ternary compounds like $Cu_4Mo_6S_8$ reach $24e^-$ counting per cluster unit. By filling up the valence band with $24e^-$ a semiconductor is obtained with an energy gap calculated to range between 0.11-0.13 Ry (1.49-1.76 eV) [19]. For $Mo_{4.2}Ru_{1.8}Se_8$, this energy gap was determined to be 1.3 eV [9]. The distribution of d-state density is shown in Fig. 2 [20].

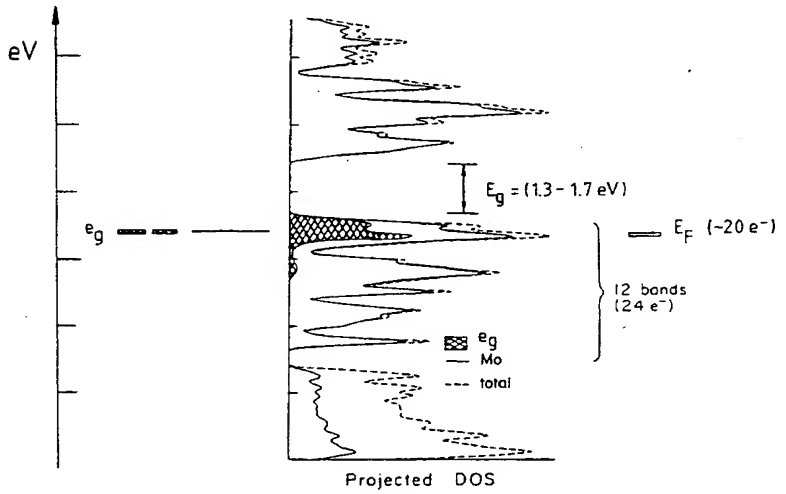

Fig. 2. Projected Density of States (DOS) of the Mo_6S_8 unit. The Fermi level (20 e^-) was adjusted to 1/6 of the surface belonging to 24 e^-. (adapted from ref 20).

An important crystal parameter is the angle α_R between neighbouring guest atoms within crystal channels in Fig. 1. The magnitude of this angle is correlated with the position and statistical movement of the guest atoms $P(M)_n$ (see insert in Fig.14c). In the case of Pb inserted into Chevrel phases the α_R angle is small and the position of the lead atom is fixed around a central position at P_1 (Fig. 1b). In the case of insertion of the smaller copper into a Chevrel phase, the copper atom can statistically assume 12 positions around P_1 at room temperature (Fig. 1c). The closest position of the copper atom with respect to the nearest Mo atom of the molybdenum octahedra is of the order of 3 Å, which is within metal-metal interaction. The angle α_R thus also defines the proximity of the guest atoms in the crystal channels to the transiton metal cluster. The larger the angle α_R the stronger should be the influence of guest atoms on the electronic structure of the transition metal cluster octahedra. An interesting observation can be made: Mo_6Se_8 is still

attacked by aqua regia but $Mo_4Ru_2Se_8$ and $Mo_2Re_4Se_8$ are stable against this very aggressive medium. Sulfide semiconductors with a high d-charater of the valence band such as RuS_2, $IrSe_2$ or $GaMo_4S_6$ are also found to be stable against attack by aqua regia. The discovery of transition metal sulfides which are kinetically stable against aggressive oxidation agents due to the involvement of d-state electrons provides us with a new criterion for the selection of improved catalysts for multi-electron transfer reactions. Sulfides which are stable against aqua regia are also expected to show improved stability as electrodes in electrochemical cells which is an important precondition for their use as (photo)electrocatalysts.

The condensation of an octahedrical Mo_6 cluster has conducted to new and yet largely unexplored compounds with clusters of Mo_9, Mo_{12}, Mo_{15}, Mo_{18} and so on up to infinite chains of $(Mo_{6/2})$. Substitution of transition metals with higher electron number than Mo into these clusters could theoretically also make them semiconducting. However, solid state chemical research in this field is still in its infancy.

Photoelectrochemical research on cluster materials

ReS_2 with its Re_4 clusters is a semiconductor (Eg = 1.3 eV) which is available and has been studied in a photoelectrochemical cell as a p-type as well as an n-type material [16,17]. Its anodic behaviour under illumination is dominated by a reaction with water which, due to a strong Re-O bond, leads to the formation of Re_2O_7 which is unstable in contact with water. Not all crystals grown by different vapour transport techniques show visible photoevolution of oxygen, but such crystals can be identified. ReS_2 can therefore, under assistance of an external potential, in principle photooxidize water to molecular oxygen but has an unfavourable interfacial chemistry.

Photoeffects with low quantum efficiencies have also been observed with $GaMo_4S_6$ when used as an electrode in an electrochemical cell. An energy gap of Eg = 1.3 eV has been observed. Stable anodic photocurrents were reported but their response was sluggish [13]. The photocharge turned over during these experiments (5 h in contact with 0.1M NaOH) was, however, not sufficiently high to prove stability. Photocurrent-voltage curves have also been reported for $Re_6Se_8C_{12}$ [21]. Photocurrents were studied in presence of redox systems such as I_2/I^- and an energy gap of Eg = 1.42 eV was observed for this n-type material. Small cathodic photocurrents were also observed with $Ru_{1.8}Mo_{4.2}Se_8$ in contact with electrolytes. They were sufficiently large to permit the determination of an energy gap with the magnitude of Eg = 1.3 eV [9].

EXPERIMENTAL PROCEDURE FOR ELECTROCATALYTICAL STUDIES

Experimental set-up

A standard electrochemical arrangement was employed. The cell had one compartment containing the working electrode, the reference electrode (SCE), which was connected to the cell compartment through a liquid junction bridge with a high porosity ceramic tip, a platinum ring as counter electrode, and a bubbler inlet. Here, all potentials will be referred to the Normal Hydrogen Electrode (NHE). Fig. 3 shows the experimental set up. Data control and acquisition, as well as statistical and electrochemical analysis were carried out by a PDP11 computer. The computer was programmed in such a way that repeated experiments (typically 10) were performed under steady state conditions with a subsequent statistical evaluation.

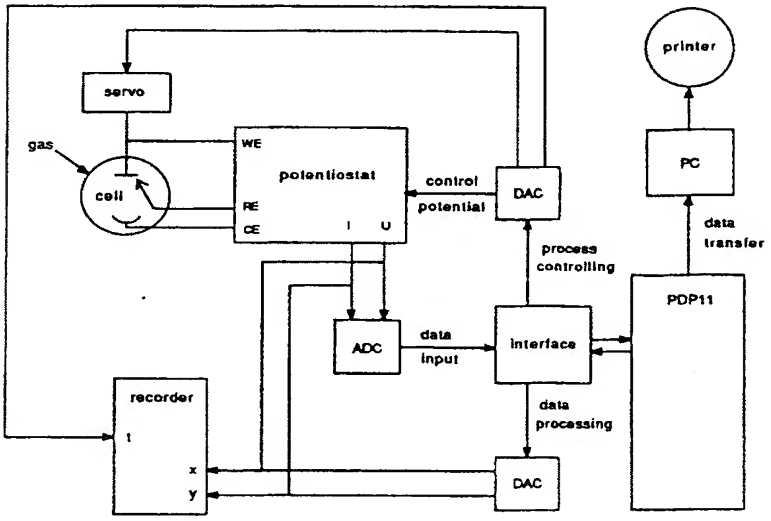

Fig. 3. Block diagram of the electrochemical measurement system. Servo: Pine Instrument; Potentiostat: Wenking POS 73; recorder: Rhode & Schwarz ZSK2; ADC and DAC: 14 and 8 HMI Model; PDP11 plus Interface: DE 85A HMI; PC: Macintosh plus-Cluster; Printer: Laser writer (M0156Z), Apple Computer Inc.

Cluster preparation

All cluster materials reported in this paper were prepared thermically. For a more detailed description of the cluster preparation the reader should be referred to the following literature. For $Mo_{4.2}Ru_{1.8}Se_8$ [9]; $Mo_4Ru_2Se_8$ and $Mo_2Re_4Se_8$[10]; $Mo_2Re_4S_8$ and $M_xMo_6S_8$ (with M(x) = Pd(1); Ag(1); In(1); Sn(1); Cd(1); Cu(2); Zn(1); Ba(1); Pb(1)) [22].

Electrode preparation

Sintered electrodes

The $Mo_{4.2}Ru_{1.8}Se_8$ cluster materials were cut from ingots of approximately 1 mm thickness, and shaped into disks on a minigrill with an abrasive paper. These disks and $Mo_4Ru_2Se_8$ pellets heated from cold pressed powder were back-ohmic contacted with a silver epoxy paste (Scotchcast 3M), and mounted on brass shafts for the rotating disk electrode (RDE) configuration.

Supported electrodes

Under this name we designate the electrodes made of (i) carbon paste substrate and (ii) polymer Nafion film on glassy carbon substrate.

(i) Carbon paste electrodes were prepared from graphite powders (Aldrich) with paraffin oil (Merck) as pasting medium (52.8 % w), as described by Adams [23]. The paste was placed in the cup of an electrode holder made of Vespel with a brass contact at the bottom. The geometrical surface of this electrode (0.25 cm^2) was smoothed by rubbing gently on a piece of weighing paper. This is the base electrode. The catalyst in powder was mixed in an agate mortar with the pasting medium (50% w). The catalytic surface was made by removing a small amount of the paste from the base electrode as uniformly as possible and refilling this part with the paste containing the catalyst. Again, the polishing of the surface was made with a piece of weighing paper. The experiments confirmed the reproducibility of such a procedure which also has the advantage of using very tiny amounts of the catalyst and testing several materials in short time.

(ii) This way of preparation was described in a preceeding publication [24]. The substrate was a disk of glassy carbon (0.07 cm^2) (kindly donated by Sigri-Elektrographit).

Analytical grade pure reagents and triply distilled water were used. The experiments were performed at room temperature.

NORMALIZATION OF THE CATALYTICAL SURFACE ACTIVITY ON SUPPORTED ELECTRODES

We have found remarkable differences concerning the background current both among and within the electrodes supported on carbon paste [25] and Nafion polymer. In order to evaluate and to compare the catalytical activity of the cluster particles, we proceeded to measure the charging current of all the samples so as to normalize their electrochemical activity. The slope deduced (differential capacity) from the charging current as a function of the scanning rate for the carbon paste and the glassy carbon Nafion covered electrode turned out to be 10 $\mu F\ cm^{-2}$ and 24 $\mu F\ cm^{-2}$,

respectively. The observation was that about 1/3 of the analyzed materials gave a differential capacity around 10 times the substrate ones. The rest gave lower or higher capacity ranging of up to 90 times the substrate (Fig. 4).

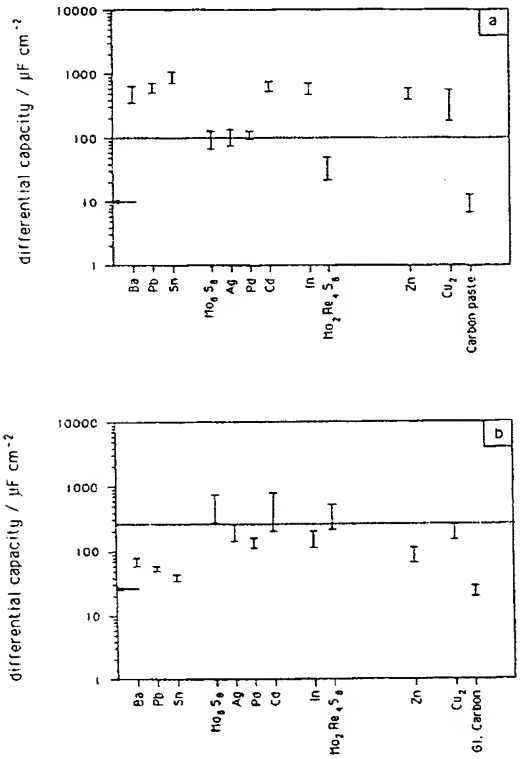

Fig. 4. Differential capacity of the cluster material particles supported on (a) carbon paste electrodes and (b) Nafion-polymer glassy carbon electrodes. Dashed lines indicate the normalizing basis adopted for each system. Small arrows show the corresponding differential capacity of the unsupported electrodes.

Experience showed that normalization of carbon paste electrodes with respect to the high measured surface areas (factor 90) leads to unrealistic high current densities for oxygen reduction. It had to be concluded that in this case the catalytically active area is not equivalent to the measured total surface area and that a 'realistic' capacity must be 10 times that of the substrate. In the case of Nafion based electrodes the statistical average could be taken which was of the same order of magnitude. Consequently, the

normalizing basis for carbon paste and Nafion polymer supported electrodes taken was 100 μF cm^{-2} and 240 μF cm^{-2}, respectively. It is interesting to mention that from 100 independent measurements performed on various carbon paste electrodes containing $Mo_2Re_4S_8$ particles, the differential capacity was found near to that of the substrate, cf. Fig. 4a. It can also be deduced that the corresponding loading of cluster particles in the Nafion-polymer film amounts to about one fourth referred to loaded carbon paste (50% w), when considering the ratio of the biggest average capacity value to that of the substrate.

OXYGEN REDUCTION STUDIES

Experiments on sintered samples

Due to the difficulty of compacting the material, few samples were tested under this form. The catalytic behaviour for the oxygen reduction in 0.5 M H_2SO_4 of Mo_6Se_8, $Mo_2Re_4Se_8$, $Mo_4Ru_2Se_8$ pellets and $Mo_{4.2}Ru_{1.8}Se_8$ melted powder clusters are shown in Fig. 5.

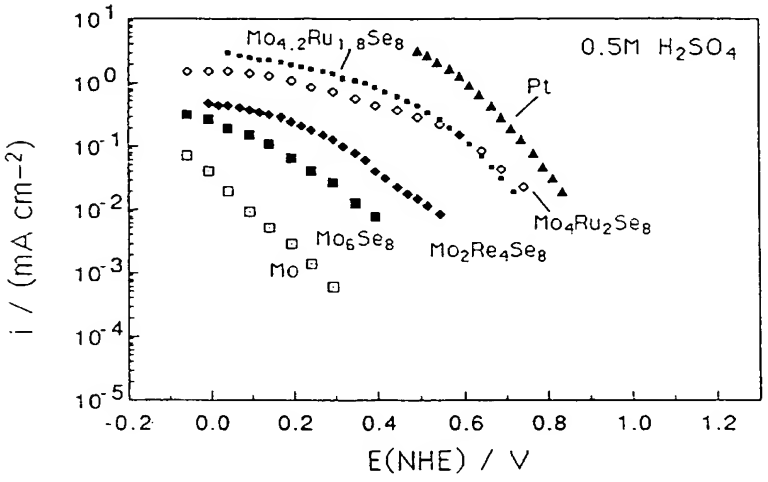

Fig. 5. Corrected mass transfer Tafel plot for molecular oxygen reduction at sintered materials Mo_6Se_8, $Mo_2Re_4Se_8$, $Mo_4Ru_2Se_8$ and $Mo_{4.2}Ru_{1.8}Se_8$, in 0.5M H_2SO_4 (pH 0.3). The data represented are those averaged from the various electrode rotation rates after the mass transfer correction. Pt and Mo metals are also represented.

The catalytic behaviour of Pt and Mo metal is indicated for comparison.
These Tafel plots demonstrate that replacement of Ru by Re in a semiconducting mixed cluster compound cannot approach the oxygen

reduction property of $Mo_4Ru_2Se_8$. However, the Re-containing mixed cluster is still more catalytic than the matrix cluster Mo_6Se_8. In the case of the Ru-containing samples with different stoichiometry the Tafel slope is different. Nevertheless, the catalytic current density remains of the same order of magnitude. $Mo_{4.2}Ru_{1.8}Se_8$ reduces O_2 to H_2O in a 4 electron reduction process with less than 4% of H_2O_2 formation [9].

Experiment on carbon paste supported electrodes

The facility that carbon paste offers to study nonconducting or conducting materials in the form of particles has allowed us to measure the catalytic activity of a variety of cluster compounds with the Mo_6S_8 matrix [25]. These compounds are Mo_6S_8, $M_xMo_6S_8$ (with M(x) = Pd(1); Ag(1); In(1); Sn(1); Cd(1); Cu(2); Zn(1); Ba(1); Pb(1)) and $Mo_2Re_4S_8$. According to the metal atom inserted in the cluster matrix, the number of electrons per cluster unit changes. For the sake of clarity we have represented the molecular oxygen reduction Tafel plots of this ensemble of materials in Fig. 6. It is clearly observed, e.g., in Fig. 6a that the activity of the compounds increases as the electron count per cluster goes from 20 in Mo_6S_8 to 24 in the Re-mixed cluster (cf. Table I) (see section 'Evaluation of kinetics and catalysis' for further discussion). In Fig. 6b, although the electron count is the same (22 e$^-$), the difference is, however, still significant. Here we observe that the ionic radius of the inserted metal between the clusters probably affects their catalytic activity. Tafel plots of the cluster materials which do not contain intercalated transition metals are separately presented in Fig. 6c. Again, the difference observed can be correlated with the size of the ionic radius of the metals, although the catalytic current remains at a low level compared to those observed in Fig. 6 (a, b).

Open circuit potentials were measured before and after molecular oxygen reduction in oxygen saturated solution. Catalyst supported electrodes showed a rapid stabilization compared to the substrate. The open circuit potential values remained stable in a time interval of 3 to 20 hours. Fig. 7a displays the results. On the other hand, the pure carbon paste electrode was not stable. All ternary cluster compounds with metal atoms between Mo clusters turned out to give a mixed potential value (cf. Fig. 11) around the open circuit potential. This correspond to an overpotential $\eta \geq 0.6V$. It is interesting to notice that a mixed cluster of Ru (sintered material) and Re supported on the carbon paste tends to approach the performance of the best catalyst (Pt) measured in the same conditions ($0.3V \leq \eta \leq 0.4V$). However, the expected catalytic trend correlating with the number of electrons per cluster with less than 24 e$^-$ (cf. Fig. 6a) is not observed in Fig. 7a. We plotted the equivalent curve at a defined current density (10^{-2} mA cm^{-2}) in Fig. 7b. An

increase of the catalytic activity is now observed. It is possible to find a better correlation between the cluster geometry and the catalytic activity, as explained later.

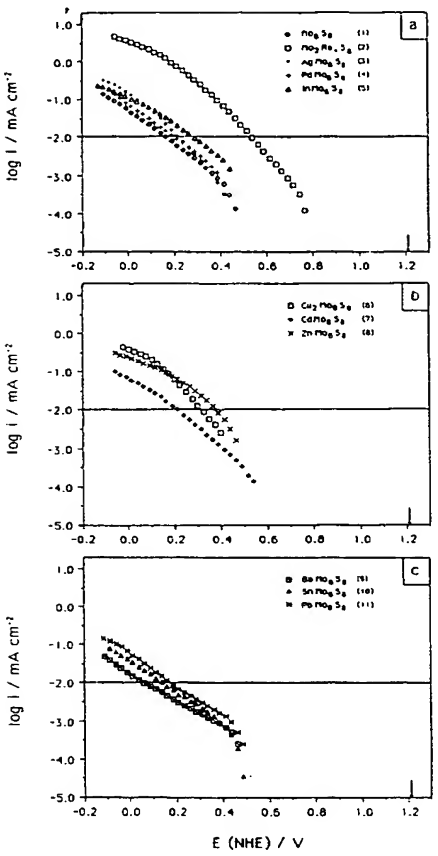

Fig. 6. Corrected mass transfer Tafel plot for molecular oxygen reduction at cluster catalysts supported in carbon paste electrodes in 0.5M H_2SO_4 (pH 0.3). The data represented are those averaged from the various electrode rotation rates after the mass transfer correction. The arrows show the thermodynamic potential for O_2 in this medium. For the description on (a), (b) and (c), see text for explanation.

This also proves that the carbon paste substrate does not play an important role in the process of oxygen reduction, since its effect is to be found at the level of the least catalytic material under normalized conditions cf. Fig. 4a. The fraction of H_2O_2 formation during O_2 reduction on paste electrodes was found to range between 2 - 12% [26].

Experiments with glassy carbon and Nafion supported electrodes

Independent of some substrate effects, the catalytic activity of catalysts particles, embedded in the Nafion-polymer film, is observed. The same trend as was demonstrated above with the carbon paste substrate was also obtained here, see Fig. 8. Some cluster compounds (containing Sn and Pb

metal atoms) did not show a significant electrochemical response in the presence of molecular oxygen compared to the Nafion substrate.

Table I. Lattice parameters for ternary and mixed cluster compounds [ref 18b, c].

Compound	NEC	α_R [°]	C_H [pm]	a_R [pm]
Mo_6S_8	20	91.27	1088.9	643
$Mo_2Re_4S_8$	24	93.43	1043.1	641
$PdMo_6S_8$	22	92.40	1068.0	644
$AgMo_6S_8$	21	91.27	1083.0	648
$InMo_6S_8$	23	93.02	1068.0	652
$Cu_2Mo_6S_8$	22	95.19	1021.9	651.8
$CdMo_6S_8$	22	92.77	1072.9	651.7
$ZnMo_6S_8$	22	94.56	1029.4	648.1
$BaMo_6S_8$	22	89.0	1170.0	664
$SnMo_6S_8$	22	89.71	1134	651
$PbMo_6S_8$	22	89.45	1143	654
Mo_6Se_8	20	91.58	1121	666
$Mo_2Re_4Se_8$	24	93.61	1074.0	663
$Mo_4Ru_2Se_8$	24	93.28	1085.0	665.7

NEC- number of electrons per cluster unit; α_R- rhombohedral angle; C_H- Hexagonal axis; a_R- rhombohedral axis.

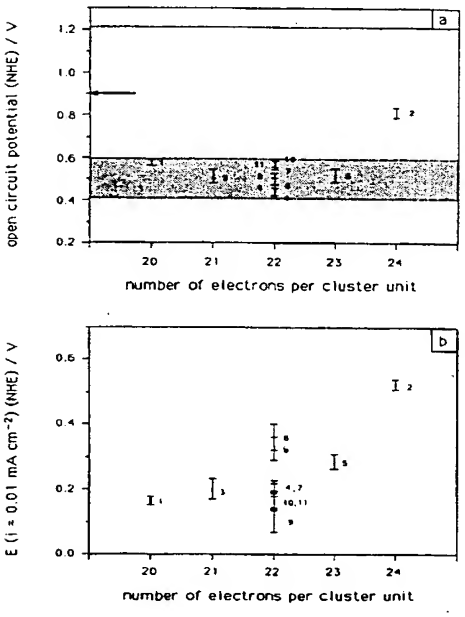

Fig. 7. (a) Open circuit potential of cluster supported on carbon paste as a function of electron count per cluster unit. (b) the same as (a) but at a potential measured at i=0.01 mA cm^{-2} (see dashed lines in Fig. 6). The numbers indicate the cluster materials also depicted in Fig. 6. The dashed line indicates the arrow shows the open circuit potential obtained with Pt under the same condition.

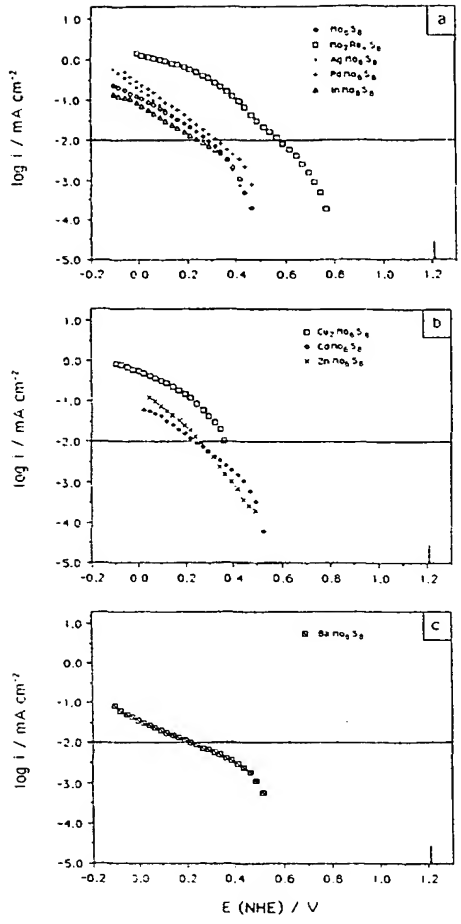

Fig. 8. Corrected mass transfer Tafel plot for molecular oxygen reduction at cluster catalysts supported on Nafion polymer electrodes in 0.5M H_2SO_4 (pH 0.3). The data represented are those averaged from the various electrode rotation rates after the mass transfer correction. The arrows show the thermodynamic potential for O_2 in this medium. For the description of (a), (b) and (c), see text.

The reason why the cluster with the metals Sn and Pb are inactive in the Nafion film is unknown to us. Certainly the type of conductivity of the substrate plays a decisive role, (cf. Fig. 4). The catalytic current obtained in the Nafion film with the active compounds is comparable to that obtained with the carbon paste substrate in spite of the tiny amounts of cluster particles present, namely, one fourth referred to the carbon paste (50% w), see 'Normalization of the catalytical surface activity on supported electrodes'. This phenomenon is not surprising, due to the high solubility of O_2 in the Nafion film which is equivalent to a significant enrichment of O_2 in this matrix [27], besides the different normalization basis employed for each system.

As regards the measured open circuit potentials before and after reduction of O_2 under oxygen saturated solution, our observations described in 'Experiments on carbon paste supported electrodes' remain essentially the same. This behaviour in open circuit condition and under a current density of 10^{-2} mA cm^{-2} is displayed in Figs. 9(a) and (b), respectively.

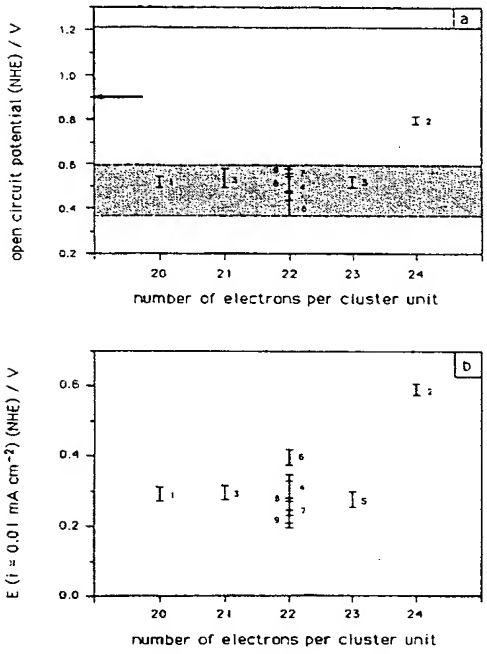

Fig. 9. (a) Open circuit potential of cluster supported on Nafion polymer as a function of electron count per cluster unit. (b) The same as (a) but at a potential measured at i=0.01 mA cm^{-2} (see dashed lines in Fig. 8). numbers indicate the cluster materials depicted in Fig. 6. The dashed line indicates the thermodynamic potential of O_2 at pH=0.3. The arrow shows the open circuit potential obtained with Pt under the same condition.

HYDROGEN EVOLUTION ON VARIOUS CLUSTER SUBSTRATES

In many metals, the cathodic hydrogen evolution process takes place with more or less significant overvoltage [28]. Platinum is here again the best catalyst given that it presents the minimum overvoltage and highest exchange current density. It was then reasonable to test and to compare the capability of the mixed cluster $(Mo,M)_6X_8$ and the ternary cluster $M_xMo_6X_8$ in order to see the influence of the electronic and structure factors for this reaction.

For the sintered cluster materials, the Tafel plot in 0.5M H_2SO_4 is displayed in Fig. 10a. For comparison, the performances of Mo metal and the pure Mo-cluster compound were also included in the same figure.

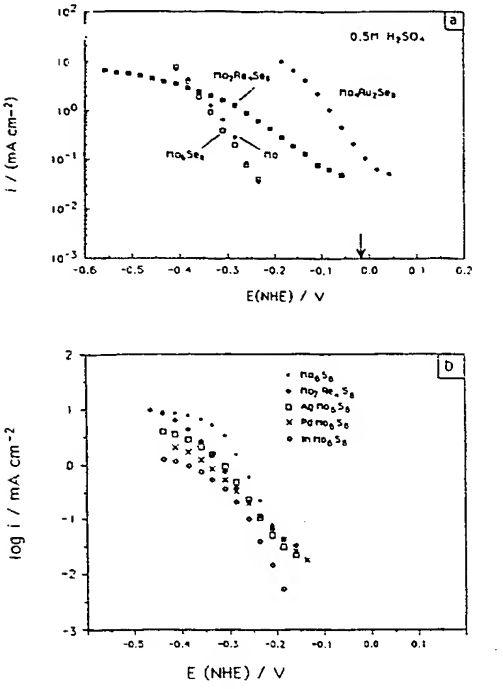

Fig. 10. Tafel plot for the hydrogen evolution (a) at the sintered Mo_6Se_8, $Mo_2Re_4Se_8$ and $Mo_4Ru_2Se_8$ electrodes, in 0.5M H_2SO_4. The Mo metal is also shown for comparison. (b) At clusters supported on carbon paste. The arrow shows the thermodynamic potential of H^+/H_2 in this medium.

These latter materials show an inferior catalytic activity with respect to the mixed Ru and Re cluster compound and we observe a negligible overvoltage with the Ru-cluster. Similar effects have also been found on the supported carbon paste and Nafion-glassy carbon electrodes. For the sake of comparison, we only show several examples carried out on the carbon paste supported electrodes in the Fig. 10(b).

Table II summarizes the kinetic (exchange current density and transfer coefficient) data for the hydrogen evolution reaction at mixed and ternary cluster compounds.

Table II. Hydrogen evolution kinetic parameters on ternary and mixed cluster compounds represented in Fig. 10.

Compound	b [mV/dec]	α	log i_0 [mA cm^{-2}]
Mo_6Se_8	73	0.81	-4.84
$Mo_2Re_4Se_8$	146	0.40	-1.70
$Mo_4Ru_2Se_8$	77	0.77	-0.85
Mo_6S_8	59	1.0	-5.0
$Mo_2Re_4S_8$	100	0.59	-3.5
$AgMo_6S_8$	77	0.77	-4.7
$PdMo_6S_8$	110	0.54	-3.2
$InMo_6S_8$	60	0.98	-5.4

CORROSION STABILITY

Most of the cluster compounds studied for the oxygen reduction and hydrogen evolution processes in supported carbon paste electrodes were tested for corrosion stability in order to compare the stability of the Mo_6S_8 cluster matrix with the ternary clusters (metal hosted in the channels) and the mixed cluster. Interesting and complicated features were obtained during the recording of this process (anodic reaction). The first and the 'stabilized' Tafel curve (which ocurred after the second or after a maximum of 10 recordings depending on the cluster compound) are displayed in Fig. 11. Qualitatively, we can distinguish that the corrosion process decreases in the following order: Pd > Cu > Ag > Sn ≈ Ba ≈ Pb > Cd > Mo_6S_8 > $Mo_2Re_4S_8$. Judging by the magnitude of the corrosion current density in the same potential interval, the Re-mixed cluster compound seems to be more stable than the cluster matrix Mo_6S_8, Fig. 11(a,b). This result is in accordance with previous ESCA surface studies made in our laboratory with the $Mo_{4.2}Ru_{1.8}Se_8$ cluster [9]. The ternary clusters present more inhomogeneous characteristics in the anodic region. This behaviour is well represented by Pd, Ag and Cu containing cluster compounds. After a moderate corrosion of these compounds, it turned out that the differential capacity and the catalytic current for the O_2 reduction was enhanced for all materials. After normalization the Pd, Ag and Sn-containing clusters still showed a significant enhancement of O_2 reduction. These experiments put in evidence that part of the metal was excalated from the matrix cluster and was catalytically reactive on the electrode surface when reduction took place. The highest first peak and the wave at more anodic potential, e.g., Fig. 11(c,d,e), obtained represent in addition to the corrosion process a topotactic reaction:

$$M_xMo_6S_8 \rightarrow M_{x-y}Mo_6S_8 + y\ M^{n+} + n\ e^- \quad (1)$$

$$M_{x-y}Mo_6S_8 + z\ H_2O \rightarrow \text{molybdate, sulfate} \quad (2)$$

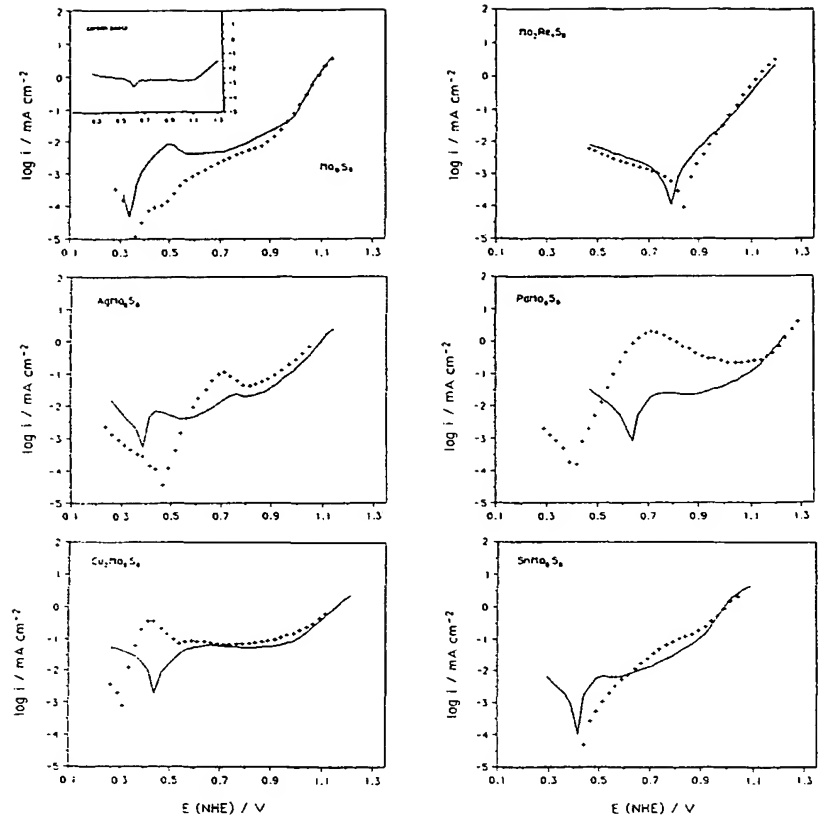

Fig. 11. Tafel corrosion curves on cluster catalysts supported on carbon paste electrodes in 0.5M H_2SO_4. (+) Shows the initial recording and (—) the 'stabilized' curve. (a) Mo_6S_8, (b) $Mo_2Re_4S_8$, (c) $AgMo_6S_8$, (d) $PdMo_6S_8$, (e) $Cu_2Mo_6S_8$, (f) $SnMo_6S_8$. The insert indicates the electrochemical behaviour of the carbon paste under the same condition.

Preliminary Rotating Ring Disk Electrode (RRDE) and X-ray in-situ measurements were performed to further analyse the interfacial mechanism due to a corrosion alteration of the catalyst surface [26]. It was found that corrosive anodic pretreatment typically leads to an increase in the rate of H_2O_2 formation during oxygen reduction. On noncorroded catalyst surfaces the proportion of H_2O_2 formation ranges between 2 - 10%. $PdMo_6S_8$, for example, shows initially 7-10% H_2O_2 formation, which after corrosion increases to 43%. Other compounds like $AgMo_6S_8$ show the same tendency. H_2O_2 production decreases during cathodic O_2 reduction because the interfacial ions move back into the bulk.

EXPERIMENTS IN NON AQUEOUS ELECTROLYTES

It can be concluded that efficient catalysis is only possible with catalyst samples which are anodically stable and that the onset of anodic corrosion is limiting the catalytic performance. This has also focussed attention on the anodic corrosion of the mixed clusters $(Mo,Ru)_6Se_8$ which in aqueous environment leads to molybdate. Preliminary experiments in non aqueous electrolytes (acetonitrile and methanol) are indeed indicating that the excellent catalytic properties of the cluster material for oxygen reduction can further be increased by slowing down and delaying anodic corrosion involving the transition metal cluster itself [29]. The catalytic properties of the cluster material for oxygen reduction is thus not limited by the catalytic parameters but by anodic corrosion and in order to fully take advantage of it, it will be necessary to select interfacial conditions which guarantee anodic stability close to the thermodynamic reduction potential of oxygen to water.

SELECTIVITY OF TRANSITION METAL CLUSTER ELECTRODES

One of the interesting problems to solve in the technology of methanol-based or other fuel cells is the selectivity of catalysts vis-à-vis the molecular oxygen reduction in the presence of organic molecules. Most of the presently known catalysts establish a mixed potential in methanol-containing electrolytes such as in the case of platinum metal. Up to now, the electrode material which seems to fulfil this requirement has been the iron-tetramethoxyphenyl-porphyrin in Teflon-bonded carbon [30].

Preliminary experiments carried out on the sintered mixed transition metal cluster ($Mo_{4.2}Ru_{1.8}Se_8$) compound in methanol-containing 0.5M H_2SO_4 electrolyte showed no generation of a mixed potential up to a methanol concentration of 3.5M. The catalytic current remained stable during the molecular oxygen reduction. Fig. 12 contrasts this behaviour together with the metallic platinum electrode in 0.5M H_2SO_4 + 1M CH_3OH. These curves were obtained with the Rotating Disk Electrode (RDE) at ω = 400 rpm. The platinum activity is very degraded as the incomplete oxidation products of methanol remain adsorbed on its surface. In this condition, the generated mixed potential attains a negative shift of 0.13 V, see curve d in Fig. 12.

Application to the methanol fuel cell

With the knowledge of the selectivity of the cluster material, we have also undertaken a preliminary study of this cathode in a methanol fuel cell.

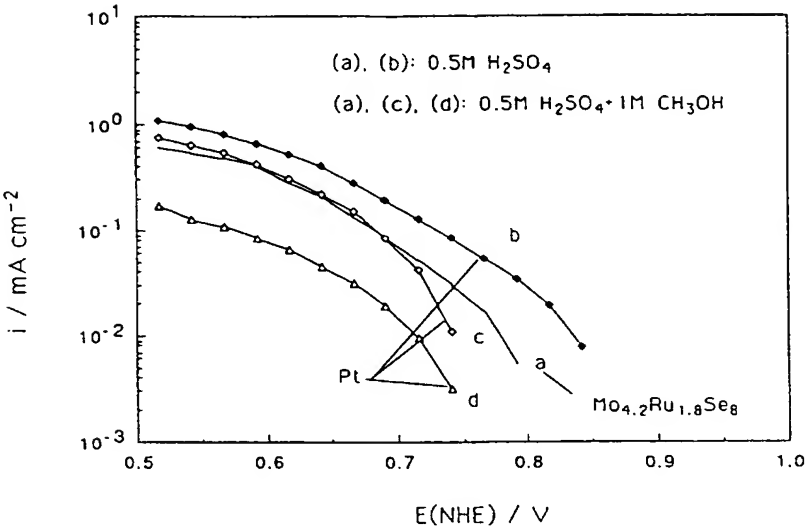

Fig. 12. Current density- potential curves for the molecular oxygen reduction obtained with the RDE at 400 rpm, in 0.5M H_2SO_4 and 0.5M H_2SO_4 +1M CH_3OH at $Mo_{4.2}Ru_{1.8}Se_8$ cluster and Pt electrodes.

As anode, we have applied the tin (upd) modified platinum reported by Watanabe et al. [31]. The cell was very simply constructed, having a glass frit of high porosity which served as a separator between the cathode and the anode compartment. Fig. 13a shows the evolution of the open circuit potential difference of the fuel cell before and after saturation of the cathode compartment with molecular oxygen. The characteristic of the same cell is represented in Fig. 13b. It is clear that the fill factor obtained is not satisfactory. However, it shows the possibility to generate an acceptable voltage cell.

EVALUATION OF KINETICS AND CATALYSIS

Due to the existing pronounced delocalization of electrons in the cluster units, it is expected that the relaxation of interfacial electronic states during electrocatalytic mechanisms would be attenuated. The consequence is that the energy levels near the Fermi level shift within a narrow energy range. In addition, the density of electronic states is high. This is especially the case when the interaction among the cluster units is relatively low, as in Chevrel phases. In these phases the density of states near the Fermi level is also favoured due to the presence of an energy gap, Fig. 2. Under these conditions

multi-electron transfer processes like the reduction of molecular oxygen to water (4 e^-) are favoured, because the change of the formal oxidation state at the reaction centers (Mo_6 octahedra) does not have a significant influence on the surface position of the electrochemical potential (Fermi level).

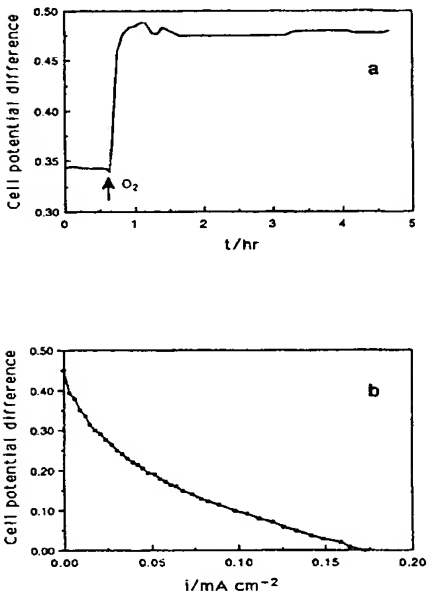

Fig. 13. (a) Cell potential difference before and after oxygen saturation of the anolyte. (b) Characteristic of the methanol acid electrolyte fuel cell. Anode: $Mo_{4.2}Ru_{1.8}Se_8$; cathode: Pt, with a Sn coverage of θ=0.63.

The existence of the cluster is equivalent to having a reservoir for electrons. Another advantage of using cluster materials is to accomplish cooperative reactions of reactants bound to neighbouring transition metal sites of the cluster.

The presence of transition metals in the cluster unit guarantees a high percentage of d-character in the energy bands near the Fermi level. A high d-state density at the edge of the valence band provides an advantage for suppressing interfacial corrosion by generating kinetic stability. In fact, experiments carried out on the binary RuX_2 (X = S, Se, Te) [32] have shown that corrosion goes in parallel with an increase of mixing Ru d-states at the edge of the valence band with the p-states of chalcogens.

On the basis of these conclusions, Chevrel phase type clusters studied here fulfil essential requirements concerning multi-electron charge transfer properties and the ability to involve interfacial coordination chemistry. In all compounds with the formula $M_xMo_6S_8$, the Mo_6 octahedron forming the

cluster unit is responsible for the high concentration of d-states. The interaction of the p-states from the intercalated metal with the cluster unit does not significantly modify the d-character of these orbitals.

However, the influence of intercalated metals on the catalytic activity of the O_2 reduction process is evident as can be observed by correlating the catalytic activity with the geometric parameters of the unit cell. The more significant parameters for this correlation which define the distortion of the unit cell are α_R and c_H. Fig. 14 shows the influence of the geometric factor α_R on the thermodynamic and kinetic parameters. In Fig. 14a, we observe no marked dependence of the open circuit potential as a function of α_R, within a range of approximately 0.2V, with exception of the mixed cluster which shows a clearly more favourably open circuit potential. This corresponds to the results presented in the Figs. 6a and 7a, in which the number of electrons per cluster unit was taken as variable. On the other hand, it is possible to observe a fairly good correlation of α_R with the kinetic parameters such as the potential at a determined current density and the Tafel slope, b, deduced from the low current density region of the curves presented in Fig. 6. The correlation of the kinetic parameters with the c_H parameter, not shown here, provides actually a mirror-image of the points displayed in Fig. 14.

The dependence of the Tafel slope on the structural parameter α_R could indicate that the mechanism of the molecular oxygen reduction is proceeding at different active sites. Based on the small amount of hydrogen peroxide produced by each cluster material (typically 2-12%), we can formulate that the reduction process of the molecular oxygen is carried out through a similar mechanism involving a peroxide-like structure as proposed recently [10]. This means that this peroxide structure developed initially on the Mo-octahedra matrix is partially rearranged with respect to the metal intercalated between the cluster, similar to the bimetallic systems. A positive or negative effect for catalysis, in terms of the interaction of the peroxide species, could be determined according to the nature of the intercalated metal within the clusters. This phenomenon can be visualized, in a step-like presentation, in Fig. 14b. Three regions are discernible, each one representing the probably equivalent mechanism of the interacting species for the corresponding cluster materials. The slopes of the Ba, Pb, and Sn-containing cluster materials vary in a significant range (220 - 350 mV/decade). The Sn-containing cluster material overlaps between the transition metals and metal-containing cluster materials. Pd, Cd, and In-containing clusters behave similarly to the matrix Mo_6 octahedra. On the other hand, the ternary clusters containing Zn and Cu behave similarly to the mixed cluster. The Tafel slope of $AgMo_6S_8$ overlaps these two regions. Aside from these observations, the trend of the

catalytic activity seems to be well defined as shown in Fig. 14c It is also observed that the ternary clusters do not approach the performance of the mixed Re-cluster either thermodynamically or kinetically cf. Fig. 14a and c, respectively.

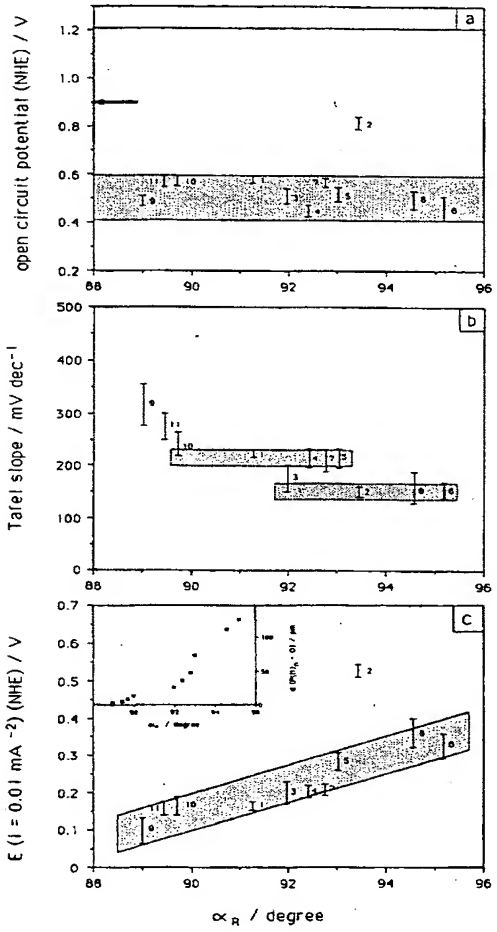

Fig. 14. Correlation of thermodynamic and kinetic parameters with the α_R parameter for the system containing cluster supported on carbon paste electrodes. Insert shows the delocalization of the intercalated metal as a function of the α_R parameter. The numbers indicate the cluster materials depicted in Fig. 6.

The catalytical electrochemical data obtained here on the ternary cluster compounds can also be correlated to the reported data obtained by low temperature neutron diffraction and by X-ray diffraction [33]. These latter techniques provided the delocalization of the intercalated metals d($P(M)_n$-O), see Fig. 1b. The bigger this distance, the closer will be the approach of the intercalated metal to the closest corner of the Mo_6 octahedron. The d($P(M)_n$-O) distance as a function of the parameter α_R is displayed in the insert of Fig. 14c showing a parallel tendency with the catalytic activity. This observation

underlines our previous conclusion that the peroxide-like bridge is associated to both the Mo_6 octahedra and a neighbouring inserted metal. For the $Cu_xMo_6S_8$, the smallest distance between Cu and Mo is about 3 Å. This could explain why the Cu-(Mo cluster) complex shows a higher activity for oxygen reduction than the Pb-(Mo cluster) complex. A limited catalytic activity as compared to the $Mo_2Re_4S_8$ can be expected due to the poor catalytic properties of Cu in association with molybdenum. In addition an unfavourable mixed electrode potential is generated because of the excalation of Cu and its chemical affinity to oxygen and water.

On the basis of our studies mixed-cluster compounds like $Mo_2Re_4S_8$ or $Mo_4Ru_2Se_8$ result to be the best catalysts: their Tafel slope is similar to the $Cu_2Mo_6S_8$ and $ZnMo_6S_8$ materials although slightly higher than the 2RT/F value. Nevertheless, their potentials at 0.01 mA cm^{-2} are much more positive than those of the ternary compounds (Fig. 14c). The reason is that the thermodynamic limit for oxygen reduction is not restricted by excalation but 'only' by oxidation of the Mo_yX_8 matrix.

Mo_6X_8 cluster compounds which also lack inserted metal atoms have inferior catalytic properties. This clearly shows that the advantage of not having excalation is not the reason for better catalyst properties but the better electronic and/or chemical factors in the mixed clusters: their Fermi levels shift towards the edge of the valence band (cf. Fig. 2) and the better catalysts have a bimetallic structure, permitting cooperative reactions on adjacent but chemically different metal sites. When the catalytic activity of cluster compounds of the composition MMo_6X_8 with metallic guest species within crystal channels is considered, it has to be taken into account both that the Fermi level is shifted towards negative potentials and an additional metal species is present which can more or less strongly interact with the molybdenum cluster (Fig. 1). The positive correlation between the α_R angle, which is dependent on the approachability to the Mo cluster by the guest atom, and on its kinetic catalytic parameters (Fig. 14) elucidates another factor which is important for catalysis: with increasing M-(Mo cluster) interaction, which produces a kind of cluster-guest metal complex, the multi-electron transfer is favoured. This positive trend is however unbalanced by the ease with which the metal species can be excalated from the crystal channels. This anodic instability does not permit to judge whether the negative shift of the Fermi level, caused by insertion of the M-species, has a positive influence on catalysis.

Results obtained with the Nafion supported electrodes in Fig. 15 are comparable to those obtained with the supported carbon paste electrodes. However, the potential measured at a current density of 0.01 mA cm^{-2} (Fig. 15c) does not show a clear increase cf. Fig. 14c.

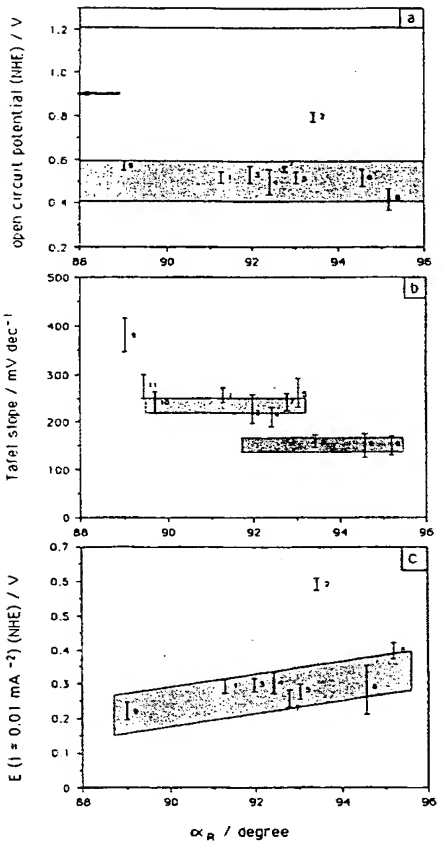

Fig. 15. Correlation of thermodynamic and kinetic parameters with the α_R parameter for the system containing cluster supported on Nafion polymer electrodes. The numbers indicate the cluster materials depicted in Fig. 6.

On the other hand, for both supported systems, although correlations of the parameters electron count per cluster unit and the ionic radius of the intercalated metal, with the electrochemical parameters exist, these are not as well defined as those obtained with α_R or $d(P(M)_n\text{-}O)$.

The influence of geometry of the cluster as well as the cluster-guest metal complex is much more pronounced on oxygen reduction than on hydrogen evolution. There is apparently less need for cooperative interaction of intermediates with the bimetallic cluster in the case of the smaller hydrogen ion.

The selectivity of the molecular oxygen reduction in the presence of methanol obtained with the mixed cluster ($Mo_{4.2}Ru_{1.8}Se_8$) compound could probably be related to the properties inferred from the electronic and geometric parameters. More research is needed to elucidate this interesting property.

CONCLUSIONS

There is a definite advantage for multi-electron catalysis, as it is needed during electrochemical energy conversion, if electronic charge carriers are channelled into bimetallic clusters for interfacial reaction with chemical species. If the electronic structure near the edges of the energy bands, where charges are transferred, has a pronounced d-character, interfacial coordination chemical mechanisms can be expected. For a successful and energetically efficient total reaction it is therefore necessary to provide the chemically adequate metallic species within the cluster entity. A key problem is the corrosion stability of the catalyst interface. Comparatively poor catalytic activity is obtained if the cluster complex is desintegrating prior to approaching the thermodynamic redox potential of the mechanism to be catalyzed. This has, for example, been the case with the Cu-(Mo cluster) complex which looses Cu through anodic extraction. The bimetallic pseudo-ternary cluster compounds are more stable and provide a high level of catalytic activity.

A key challenge for the future will be to identify bimetallic cluster compounds as well as electrolytes which provide a maximum of interfacial electrochemical stability. Already now, with molybdenum from the mixed $Mo_4Ru_2Se_8$ and $Mo_2Re_4S_8$ cluster compounds reacting with water to molybdate, a catalytic performance has been reached which approaches that of Pt for oxygen reduction in acid solution.

ACKNOWLEDGEMENT

B. Schubert thanks the Fonds der Chemischen Industrie for financial support. The authors thank Dr. E. Gocke for providing most of the materials and for helpful discussions. The work was in part supported by a grant of the BMFT.

REFERENCES

1 H. Tributsch, in J. O'M Bockris, B. E. Conway and R. E. White (eds.) Modern Aspects of Electrochemistry, Plenum Press, New York- London, 1986, Vol. 17, p. 303.
2 H. Tributsch, J. Photochem., 29 (1985) 89.
3 H. Tributsch, NATO Adv. Studies, New Trends and Applications of Photoelectrochemistry for Enviromental Problems, Palermo, Italy, Reidel Dordrecht-Boston-London, 1988, p. 297.
4 E. L. Muetterties and M. J. Krause, Angew. Chem., 95 (1983)135.
5 R. M. Laine, J. Mol. Cat., 14 (1982) 127.
6 J. S. Bradley, J. Am. Chem. Soc., 101 (1979) 7419.

7 W. Walker and J. P. Cropley, Union Carbide Corp. US Pat. 3940432 (1976).

8 N. Alonso Vante and H. Tributsch, Nature(London), 323 (1986)431.

9 N. Alonso Vante, W. Jaegermann, H. Tributsch, W. Hönle and K. Yvon, J. Am. Chem. Soc., 109 (1987) 3251.

10 N. Alonso Vante, B. Schubert, H. Tributsch and A. Perrin, J. Catal., 112 (1988) 384.

11 D. L. Kepert, The Early Transition Metals, Academic Press, London, N. Y., 1972.

12 G. B. Ansel and L. Katz, Acta Cryst., 21 (1966) 482.

13 M. Paranthanam, Thesis dissertation, Indian Institute of Technology, Madras, India, (1988).

14 R. Chevrel, Thesis Dissertation, Rennes (1974).

15 C. Perrin, R. Chevrel and M. Sergent, C. R. Acad. Sci., 280C (1975) 949.

16 B. L. Wheeler, J. K. Leland and A. J. Bard, J. Electrochem. Soc., 133 (1986) 358.

17 B. Schubert and H. Tributsch, J. Electrochem. Soc., submitted for publication.

18 (a) K. Yvon, in Ø. Fischer and M. B. Maple (eds.) Superconductivity in Ternary Compounds, Springer Verlag, Berlin, 1982, p. 87.
(b) W. Hönle, H. D. Flack and K. Yvon, J. Solid State Chem., 49 (1983) 157; (c) R. Chevrel and M. Sergent, in Ø. Fischer and M. B. Maple (eds.) Superconductivity in Ternary Compounds, Springer Verlag, Berlin, 1982, p. 25.

19 L. F. Mattheiss and C. Y. Fong, Phys. Rev. B, 15 (1977)1760.

20 T. Hugbanks and R. Hoffmann, J. Am. Chem. Soc., 105 (1983) 1150.

21 N. Le Nagard, A. Perrin, M. Sergent and C. Lévy-Clement, Mat. Res. Bull., 20 (1985) 835.

22 (a) E. Gocke, R. Schöllhorn, G. Aselmann and W. Müller-Warmuth, Inorg. Chem., 26 (1987)1805; (b) E. Gocke, R. Schöllhorn, in preparation.

23 R. N. Adams, Electrochemistry at Solid Electrodes, Marcel Dekker, New York, Basle, 1969, p.281.

24 N. Alonso Vante and H. Tributsch, J. Electroanal. Chem., 229 (1987) 223.

25 B. Schubert, N. Alonso Vante, E. Gocke and H. Tributsch, Ber. Bunsenges. Phys. Chem., in press.

26 B. Schubert, N. Alonso Vante, H. Tributsch, E. Gocke and R. Schöllhorn, in preparation.

27 S. Gottesfeld, I. D. Raistrick and S. Srinivasan, J. Electrochem. Soc., 134 (1987)1455.

28 K. J. Vetter, Electrochemical Kinetics, Theoretical and Experimental Aspects, Academic Press, New York-San Francisco-London, 1967, p. 537.
29 M. Bungs, N. Alonso Vante and H. Tributsch, in preparation.
30 R. Holze, I. Vogel and W. Vielstich, J. Electroanal. Chem., 210 (1986) 277.
31 M. Watanabe, N. Furuuchi and S. Motoo, J. Electroanal. Chem., 191 (1985) 367.
32 H.-M. Kühne, W. Jaegermann and H. Tributsch, Chem. Phys. Lett., 112 (1984)160.
33 K. Yvon, in E. Kaldis (ed.) Current Topics in Materials Science, North Holland, Amsterdam, 1979, Vol. 3, p. 55.